

Preparation of Ni/TiO₂ Nanoparticles and Their Catalytic Performance on the Thermal Decomposition of Ammonium Perchlorate

LI, Cheng^a(李成) MA, Zhenye^{*,a,b}(马振叶)
ZHANG, Lixiong^a(张利雄) QIAN, Renyuan^a(钱仁渊)

^a State Key Laboratory of Materials-oriented Chemical Engineering, Nanjing University of Technology, Nanjing, Jiangsu 210009, China

^b College of Chemistry and Environment Science, Nanjing Normal University, Nanjing, Jiangsu 210097, China

Metal/oxide nanoparticles are attractive because of their special structure and better properties. The Ni/TiO₂ nanoparticles were prepared by a liquid phase chemical reduction method in this paper. The obtained-products were characterized by inductively coupled plasma (ICP), X-ray diffraction (XRD), high-resolution transmission electron microscopy (HRTEM) and scanning electron microscopy (SEM). The results show that Ni particles in Ni/TiO₂ nanoparticles exhibit better dispersion and the size of most Ni particles is 10 nm or so. The catalytic activity of Ni/TiO₂ nanoparticles on the thermal decomposition of ammonium perchlorate (AP) was investigated by simultaneous thermogravimetry and differential thermal analysis (TG-DTA). Results show that composite process of Ni and TiO₂ can improve the catalytic activity of Ni nanoparticles on the thermal decomposition of AP, which is mainly attributed to the improvement of Ni dispersion in Ni/TiO₂ nanoparticles. The catalytic activity of Ni/TiO₂ nanoparticles increases with increasing the weight ratio of Ni to AP.

Keywords Ni/TiO₂ nanoparticle, catalytic activity, ammonium perchlorate, thermal decomposition

Introduction

Ammonium perchlorate (AP) is the most common oxidant in composite solid propellants, and its thermal decomposition characteristics directly influence the combustion behavior of the solid propellant.¹ In recent years, the nano-sized catalysts used for the solid propellants have continuously attracted more interest due to their better catalytic activity.¹⁻⁸ The catalyst style varies from nano-size metal oxide including Fe₂O₃, CuO and Y₂O₃²⁻⁴ to nano-sized metal powder including Ni, Cu-Mg and Ni-Cu.⁵⁻⁸ Ni nanoparticles exhibit higher catalytic activity on the thermal decomposition of AP owing to their smaller size and larger specific surface.^{5,6} Unfortunately, unprotected Ni nanoparticles are susceptible to irreversible aggregation in solution due to small size and magnetism, which will lower their catalytic activity. One of effective strategies is to support metals on a proper oxide support, which can prevent aggregation.⁹

It is well known that oxide-supported metal catalysts are a very important class of industrial catalysts that are closely related with many key technologies in chemical/petrochemical industries, environmental protection, chemical sensors and the manufacture of fine and spe-

cial chemicals.¹⁰ The metal-support interactions can affect both catalytic activity and stability.^{11,12} TiO₂ is a reducible metal oxide with several crystal structures and oxidation states. Ni/TiO₂ catalysts have been used for converting methane into syngas,¹³ carbon monoxide hydrogenation¹⁴ and *p*-nitrophenol hydrogenation.¹⁵ However, in the propellant and explosive field, few researches about this kind of metal/oxide nanocomposite have been reported.

In this study, the Ni/TiO₂ nanoparticles were prepared by supporting Ni nano-particles on a size-comparable TiO₂ support. The composition, structure and morphology of the as-prepared Ni/TiO₂ nanoparticles were characterized by ICP, XRD, HRTEM and SEM. The catalytic activity of Ni/TiO₂ nanoparticles on the thermal decomposition of AP was investigated by DTA and TG. Especially, the catalytic activity of Ni/TiO₂ was compared with those of the pure Ni and TiO₂. In addition, the content effect of Ni/TiO₂ nanoparticles on the decomposition of AP was also discussed. It is found that composite process of Ni and TiO₂ can improve the catalytic activity of Ni nanoparticles on the thermal decomposition of AP. The catalytic activity of Ni/TiO₂ nanoparticles increases with increasing the weight ratio

* E-mail: mzynjust@163.com; Tel.: 0086-025-83598233

Received March 11, 2009; revised April 17, 2009; accepted June 18, 2009.

Project supported by the National Natural Science Foundation of China (No. 50702025), the Natural Science Foundation of the Jiangsu Higher Education Institutions of China (No. 08KJB430009), the Natural Science Foundation of Jiangsu Province (No. BK2009473) and Start up Foundation of Nanjing Normal University (No. 2008103XGQ0051).

of Ni to AP. The mechanism was also discussed in detail.

Experimental

Catalyst preparation

The Ni/TiO₂ nanoparticles were prepared by a liquid phase chemical reduction method.¹⁶ 1 g of TiO₂ powder (Degussa P25 with anatase/rutile crystalline ratio of 8 : 2 and surface area of 50 m²/g) was impregnated into 20 mL of NiSO₄ solution (0.25 mol·L⁻¹) under vigorous stirring at room temperature for 1 h. Then the resulting suspension was heated at 80 °C and stirred for 30 min. At last, 35 mL of N₂H₄·H₂O ($n_{\text{N}_2\text{H}_4\cdot\text{H}_2\text{O}}/n_{\text{Ni}^{2+}}=1.5$) and NaOH ($n_{\text{NaOH}}/n_{\text{Ni}^{2+}}=1.5$) mixture solution were added into the resulting suspension. The suspension was stirred for 15 min. Then the obtained suspension was washed thoroughly with distilled water and subsequently with 99.9% alcohol (EtOH). Pure Ni was prepared according to the above method without addition of TiO₂ support.

The procedure of simply mixing catalyst (Ni, TiO₂ and Ni/TiO₂) and AP was as follows: a certain amount of catalyst was ground with AP in some alcoholic solution in an agate mortar, and then dried under vacuum at room temperature.

Catalyst characterization

The composition of the Ni/TiO₂ nanoparticles was analyzed by inductively coupled plasma spectrophotometry (ICP), on a Perkin-Elmer Optima 2000DV instrument after extraction with nitric acid.

The structures of the as-prepared samples were determined by X-ray diffraction (XRD), on a Bruker D8 advance instrument using Cu K α radiation ($\lambda = 0.154178$ nm) from 20° to 80° (in 2θ) with the scanning rate of 3° per min.

The micrograph of the Ni/TiO₂ nanoparticles was determined by scanning electron microscopy (SEM), carried out on a JSM-6300 scanning electron microscope. High-resolution transmission electron microscopy (HRTEM) was also employed to investigate the morphology of the samples, on a JEOL TEM-2100 transmission electron microscope.

The catalytic activity of the as-prepared samples on the thermal decomposition of AP was measured by simultaneous thermogravimetry and differential thermal analysis (TG-DTA), with a Netzsch STA 409PC thermal analyzer at a heating rate of 20 K/min from room temperature to 500 °C in N₂ atmosphere and under ambient atmospheric pressure.

Results and discussion

Catalyst characterization

The ICP results show that the weight ratio of Ni to TiO₂ is 29.8%. Figure 1 shows the XRD patterns of pure

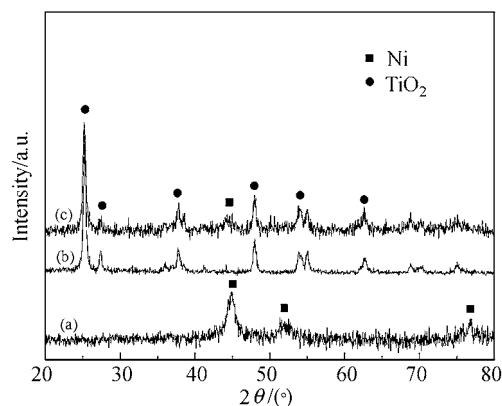


Figure 1 XRD patterns of samples. (a) Pure Ni nanoparticles, (b) TiO₂ nanoparticles, and (c) Ni/TiO₂ nanoparticles.

Ni, TiO₂ and Ni/TiO₂. The XRD pattern of the Ni nanoparticles is shown in pattern (a). Only three characteristic peaks of face centered cubic (f.c.c.) nickel ($2\theta = 44.8^\circ, 52.2^\circ$ and 76.8°) marked by Miller indices (111), (200) and (220) are observed in the 2θ range from 20° to 80°, which reveals that the as-prepared sample is pure f.c.c. nickel. The average particle size of Ni nanocrystals is 8.0 nm determined from the XRD pattern parameters of the Ni (111) according to the Scherrer equation.¹⁷ The XRD pattern of the TiO₂ nanoparticles is shown in pattern (b). The characteristic peaks of anatase and rutile crystals of TiO₂ can be seen obviously. Wherein, peaks of $2\theta = 27.5^\circ, 53.8^\circ$ and 62.8° marked by Miller indices (110), (210) and (002) belong to the rutile crystal, and the others peaks of $2\theta = 25.3^\circ, 37.8^\circ$ and 48.1° marked by Miller indices (101), (004) and (200) belong to the anatase TiO₂. In the pattern (c) of Ni/TiO₂, various crystalline diffraction peaks corresponding to crystalline TiO₂ are observed, but the characteristic peak of crystalline Ni (typically with $2\theta = 44.8^\circ$) marked by Miller index (111) is observed. The XRD measurements show no evidence for any possible compound formation between Ni and TiO₂ in the sample, which shows that the structures of TiO₂ are well preserved and the Ni(0) particles exist stably. The average particle size of Ni in Ni/TiO₂ sample is 11.6 nm according to the Scherrer equation.

The representative SEM images of Ni nanoparticles and Ni/TiO₂ nanoparticles are shown in Figure 2. As shown in Figure 2, the dispersion of Ni particles in the two samples is distinctly different. In Figure 2a, it can be seen that the Ni particles are aggregated together. The tendency of aggregation makes single Ni nanoparticles hard to be observed. In Figure 2b, although the Ni and TiO₂ particles can not be discerned at this magnification, the Ni/TiO₂ nanoparticles show more loose structures and Ni/TiO₂ nanoparticles are better dispersed.

The size and dispersion of the Ni/TiO₂ nanoparticles were also measured by HRTEM and one typical photograph is shown in Figure 3. Small particles represent clusters of the active Ni metal and large particles repre-

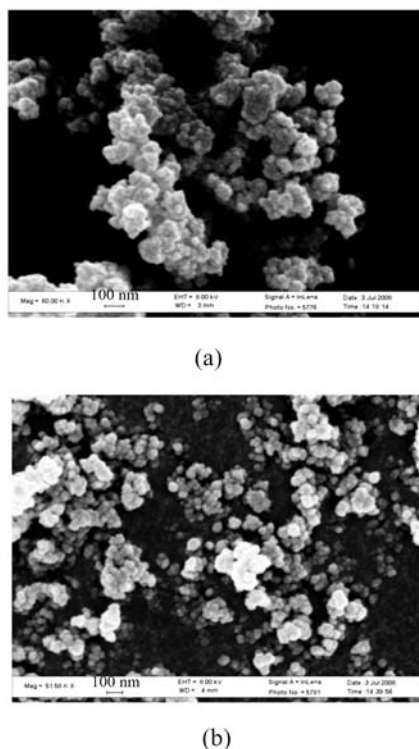


Figure 2 SEM images of (a) pure Ni nanoparticles and (b) Ni/TiO₂ nanoparticles.

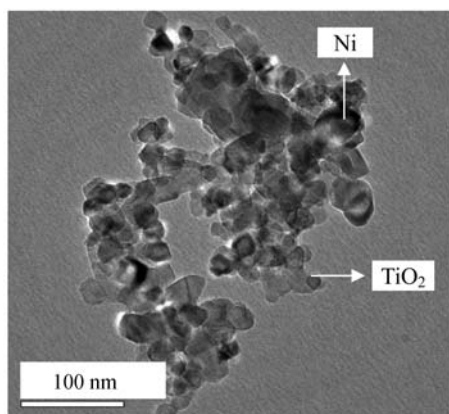


Figure 3 HRTEM image of Ni/TiO₂ nanoparticles.

sent TiO₂ particles. As shown in Figure 3, the active metal clusters are clearly visible and are homogeneously dispersed on the surface of TiO₂ particles. The size of most Ni is 10 nm or so.

Effect of composite processing of Ni and TiO₂ on the thermal decomposition of AP

To assess the effect of composite processing of Ni and TiO₂ on their catalytic activity on the thermal decomposition of AP, four samples including pure AP, AP in the presence of TiO₂ (weight ratio TiO₂ : AP=2%), AP in the presence of Ni nanoparticles (weight ratio Ni : AP=2%) and AP in the presence of Ni/TiO₂ nanoparticles (weight ratio Ni : AP=2%) were pre-

pared. The DTA and TG results for these samples are shown in Figures 4 and 5.

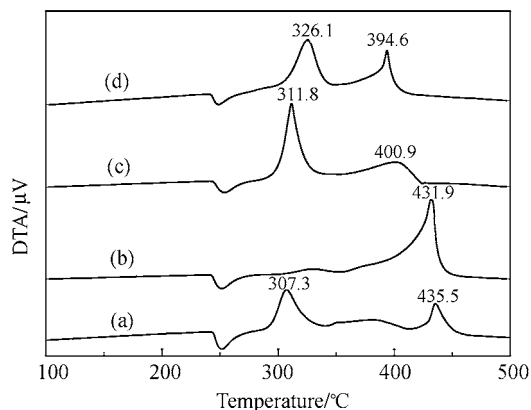


Figure 4 DTA curves for decomposition of different AP samples. (a) Pure AP, (b) AP+TiO₂, (c) AP+Ni, and (d) AP+Ni/TiO₂ nanoparticles.

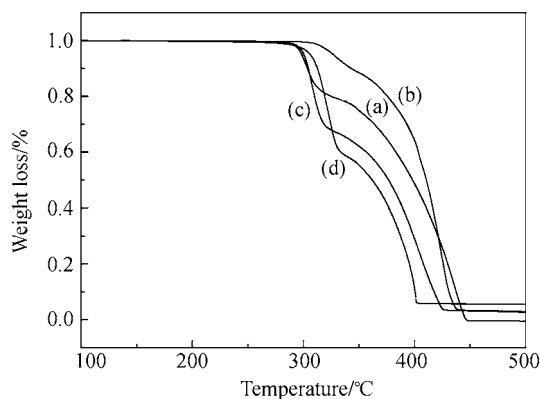
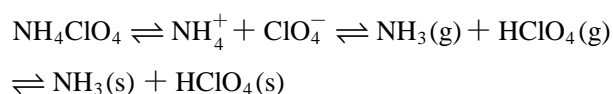


Figure 5 TG curves for decomposition of different AP samples. (a) Pure AP, (b) AP+TiO₂, (c) AP+Ni, and (d) AP+Ni/TiO₂ nanoparticles.

From Figure 4, we notice that the DTA curve for thermal decomposition of pure AP shows three events. The endothermic DTA peak at 253.8 °C represents the transition from orthorhombic to cubic AP. There are two exothermic peaks on DTA curve of pure AP, which are at 307.3 and 435.5 °C. These two peaks are denoted as low-temperature exothermic peak and high-temperature exothermic peak, respectively. The low exothermic peak corresponds to the partial decomposition of AP and the formation of an intermediate. During this process, decomposition and sublimation would first take place as follows:



Then, the degradation of HClO₄(g) and the oxidation of NH₃(g) by the products of HClO₄(g) degradation would happen. The high exothermic peak corresponds

to the complete decomposition of the intermediate products to volatile products. Both oxidation of NH_3 by ClO_4^- in gas phase and decomposition of AP on solid surface would take place in this step.¹⁸

However, the DTA curves for decomposition of AP in the presence of pure TiO_2 , pure Ni and Ni/ TiO_2 nanoparticles show noticeable differences in the decomposition patterns of AP. The endothermic peak nearby 253 °C appearing in all samples exhibits similar shape, indicating that additives have little effect on the crystallographic transition temperature of AP. However, dramatic changes for the exothermic peaks of AP decomposition have been observed for all samples.

In curve b, it is found that the low-temperature exothermic peak of AP in the presence of TiO_2 is shifted to higher temperatures and the high-temperature exothermic peak has a little change, which means that TiO_2 shows little catalytic activity on the thermal decomposition of AP. In curve c, the high-temperature exothermic peak of AP in the presence of Ni is shifted to lower temperature, which indicates pure Ni exhibits catalytic activity on the thermal decomposition of AP effectively. Whereas in the case of Ni/ TiO_2 nanoparticles (curve d), Ni lowers the peak temperature of high temperature decomposition of AP by 40.9 °C, which means that Ni in Ni/ TiO_2 nanoparticles can further lower the peak temperature of high temperature decomposition of AP by 6.3 °C with the same weight ratio of Ni to AP. The results indicate that composite processing of Ni and TiO_2 nanoparticles can improve the catalytic activity of Ni nanoparticles. The Ni/ TiO_2 nanoparticles exhibit the best catalytic activity on the thermal decomposition of AP.

The TG curves for pure AP, AP in the presence of TiO_2 , AP in the presence of Ni nanoparticles and AP in the presence of Ni/ TiO_2 nanoparticles are shown in Figure 5. All the samples exhibit two weight loss steps, corresponding to the exothermic peaks of the DTA curves. The onsets of thermal decomposition of the four samples are all at about 289 °C, while the end temperatures are about 449, 440, 427 and 403 °C, respectively. The sequence of thermal decomposition speed of these samples is as follows: AP in the presence of Ni/ TiO_2 nanoparticles > AP in the presence of pure Ni > pure AP in the presence of TiO_2 > AP. In addition, the weight loss of AP in the presence of Ni/ TiO_2 nanoparticles at low-temperature decomposition is the biggest, indicating that composite process of Ni and TiO_2 can make more AP be decomposed at the low-temperature decomposition stage.

Combining the above results, although TiO_2 exhibits nearly little catalytic activity on the thermal decomposition of AP, the composite process of Ni and TiO_2 may play an important role in the improvement of catalytic activity of Ni nanoparticles on the thermal decomposition of AP.

Effect of the weight ratio of Ni to AP on the decomposition of AP

The effect of the weight ratio of Ni to AP on the decomposition of AP was also investigated. Four samples of AP in the presence of Ni/ TiO_2 nanoparticles were prepared, in which the weight ratios of Ni to AP are 1%, 2%, 4% and 6%, respectively. The results are shown in Figure 6. It can be seen that with weight ratio of Ni to AP increasing from 1% to 6%, the peak temperatures of high temperature decomposition of AP obviously decrease by 26.3, 40.7, 52.4 and 73.0 °C, respectively, indicating that the thermal decomposition rate of AP is accelerated with increasing the weight ratio of Ni to AP.

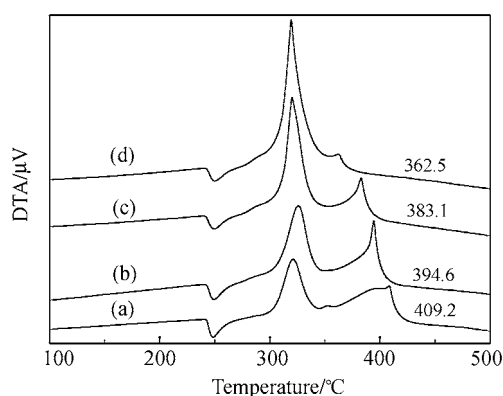


Figure 6 DTA curves for decomposition of AP as catalyzed by Ni/ TiO_2 nanoparticles with different weight ratios of Ni to AP. (a) 1%, (b) 2%, (c) 4%, and (d) 6%.

It was proposed that the rate of controlling step in thermal decomposition of AP was the electron transfer from ClO_4^- to the NH_4^+ .¹⁹ That is to say, catalyst which can provide a bridge for the transfer of electrons from the ClO_4^- to the NH_4^+ , can accelerate the decomposition rate of AP. According to this theory, the reductive capability of TiO_2 is not enough for the transfer of electrons from the ClO_4^- to the NH_4^+ , although TiO_2 is a reducible metal oxide with several crystal structures and oxidation states.

Nano-sized Ni crystal contains many defects over crystal lattice. Atoms on the defects are not saturated and tend to become steady by absorbing electrons onto its surface. Ni nanoparticle provides a bridge for the transfer of electrons from the ClO_4^- to the NH_4^+ , which makes the activation energy of thermal decomposition reduced, so the decomposition temperature of AP is decreased and the decomposition rate of AP accelerated. The Ni/ TiO_2 nanoparticles exhibit the best catalytic activity on the decomposition of AP, which may be mainly attributed to the improvement of Ni dispersion in Ni/ TiO_2 nanoparticles.

Conclusion

The Ni/ TiO_2 nanoparticles were prepared and their catalytic activities on the thermal decomposition of AP

were also investigated. The results show that Ni particles in Ni/TiO₂ nanoparticles exhibit better dispersion and the size of most Ni metal is 10 nm or so. XRD measurements show no new material formation between Ni and TiO₂. The composite process of Ni and TiO₂ can improve the Ni catalytic activity on the thermal decomposition of AP, which is attributed to the improvement of Ni dispersion. Increasing the content of Ni/TiO₂ nanoparticles can improve the catalytic activity of Ni/TiO₂ nanoparticles on the thermal decomposition of AP.

References

- 1 Liu, T.; Wang, L. S.; Yang, P.; Hu, B. Y. *Mater. Lett.* **2008**, *62*, 4056.
- 2 Bakhman, N. N.; Nikiforov, V. S.; Avdyunin, V. I.; Fogelzang, A. E.; Kichin, Y. S. *Combust. Flame* **1974**, *22*, 77.
- 3 Singn, N. B.; Ojha, A. K. *Thermochim. Acta* **2002**, *390*, 67.
- 4 Chen, W. F.; Li, F. S.; Liu, L. L.; Li, Y. X. *J. Rare Earth.* **2006**, *24*, 543.
- 5 Jiang, Z.; Li, S. F.; Zhao, F. Q. *Propellant, Explos., Pyrotech.* **2006**, *31*, 139.
- 6 Liu, L. L.; Li, F. S.; Zhi, C. L.; Song, H. C.; Yang, Y. *Acta Chim. Sinica* **2008**, *66*, 1424 (in Chinese).
- 7 Cui, P.; Zhou, J.; Jiang, W. *Propellants, Explos., Pyrotech.* **2006**, *31*, 452.
- 8 Said, A. A.; Qasmi, R. A. *Thermochim. Acta* **1996**, *275*, 83.
- 9 Xu, B. Q.; Wei, J. M.; Yu, Y. T.; Li, Y.; Li, J. L.; Zhu, Q. M. *J. Phys. Chem. B* **2003**, *107*, 5203.
- 10 Wei, J. M.; Xu, B. Q.; Sun, K. Q.; Li, J. L.; Zhu, Q. M. *Chem. J. Chin. Univ.* **2002**, *23*, 2106 (in Chinese).
- 11 Braford, M. C.; Vannice, M. A. *Appl. Catal. A* **1996**, *142*, 73.
- 12 Erdohelyi, A.; Cserenyi, J.; Solymosi, F. *J. Catal.* **1993**, *141*, 287.
- 13 Braford, M. C. J.; Vannice, M. A. *J. Catal.* **1998**, *173*, 157.
- 14 Vannice, M. A.; Garten, R. L. *J. Catal.* **1979**, *56*, 236.
- 15 Chen, R. Z.; Du, Y.; Xing, W. H.; Xu, N. P. *Chin. J. Chem. Eng.* **2006**, *14*, 665.
- 16 Ma, Z. Y.; Li, F. S.; Bai, H. P. *Propellant, Explos., Pyrotech.* **2006**, *31*, 447.
- 17 Ciambelli, P.; Cimino, S.; Rossi, D. S.; Faticanti, M.; Lisi, L.; Minelli, G.; Pettiti, I.; Porta, P.; Russo, G.; Turco, M. *Appl. Catal. B* **2000**, *24*, 243.
- 18 Duan, G. R.; Yang, X. J.; Chen, J.; Huang, G. H.; Lu, L. D.; Wang, X. *Powder Technol.* **2007**, *172*, 27.
- 19 Bircumshaw, L. L.; Newman, B. H. *Proc. Roy. Soc.* **1954**, *227*, 115.

(E0903111 Zhao, X.)